Influence of Stack Hybrid Configuration of MoS$_2$ and Graphene on the Performance of Surface Plasmon Resonance Biosensor

Amir Davami[1] (iD), Mohammd Hadi Shahrokh Abadi[2]* (iD)

[1, 2] Faculty of Electrical and Computer Engineering, Hakim Sabzevari University, Sabzevar, Iran
E-mail: mhshahrokh@hsu.ac.ir

Abstract — This paper investigates the influence of various configurations and flakes of: i) graphene, ii) graphene/MoS$_2$/graphene and iii) MoS$_2$/graphene/ MoS$_2$ over a thin layer of gold on the performance of a surface plasmon resonance (SPR) biosensor. The reflectance curves of the proposed SPR biosensor are obtained, analyzed and compared for different combinations and thicknesses of the biosensors' layers in refractive indices (RI) of 1 and 1.02, resembling an air and a bacterial medium, respectively. An in-depth analysis based on finite difference time domain method is performed to describe the sensor response considering sensitivity, full width at half maximum and minimum reflectance. The obtained results show that the sensitivity of the biosensor with a 50 nm Au and a 5 nm TiO$_2$ (as the adhesive layer between the Au- layer and the prism) is equal to 61°/RIU. In order to increase further the sensitivity, different stacks and thicknesses of MoS$_2$/graphene/MoS$_2$ and graphene/MoS2/graphene configurations on the Au layer are added. The achieved outcomes reveal that the sensitivity is improved for a monolayer of MoS$_2$ (1L_MoS$_2$) sandwiched between double layers of graphene (2L_G) on 50 nm Au and 5 nm TiO$_2$ (1L_MoS$_2$/2L_G/1L_MoS$_2$/50nmAu/5nmTiO$_2$/Prism-BK7). This combination yields a sensitivity of 71.5 °/RIU for RI changes in the sensing medium (Δn) of 0.02 with a great detection accuracy of 0.33. We hope that – based on the outcomes of this investigation - the proposed structures can open new windows to improve the SPR biosensor detection of biological species.

Keywords — Biosensor; Surface plasmon resonance; Graphene; MoS$_2$; Bacteria; Sensitivity; Lumerical environment.

1. INTRODUCTION

Surface plasmon resonance (SPR) is an optical method for detecting changes in the refractive index (RI) between a layer of metal (usually gold) and a dielectric medium [1]. Due to the importance of detecting enzymes and identifying pathogens, such structures are used in the medical and pharmaceutical fields. The surface plasmon wave was first reported by Wood in 1902, but the resonance properties of surface plasmon were unknown until Kretschmann and Otto realized it in 1968 [2]. Then, many attempts were made to use this phenomenon in various applications as a very powerful tool for determining the specifications of molecular interactions in liquids and solids. Plasmon is defined as the quantum of collective oscillations of free electrons in a metal and the surface plasmon is the electromagnetic waves emitted in the metal-dielectric interface [1, 3].

The SPR structure consists of three main parts: the optical system, the electronic system, and the data collection system. The main difference in SPR structure is more in the way of surface plasmon excitation, input light coupling with sensitive layer and output light modulation [3, 4]. There are some common methods for surface plasmon excitation including prism coupling and grating coupling [4, 5]. The most common SPR structure is based on an input light coupling with a prism, and this type of optical coupling is used in many

laboratories and even commercial models due to its simplicity. The prism coupling is presented with two different configurations: Kretschmann and Otto [6]. It is more than two decades that the Kretschmann configuration - in which a thin film of metal is deposited onto the prism surface - has been considered by the scientists for manufacturing the SPR-based biosensors and biodevices [7, 8]. These sensors are considered as the type of optical sensors that measure different biological and chemical parameters based on the interaction of the sample environment with the sensor surface by monitoring RI change of surrounding media [4]. The most important applications of these biological sensors include the detection of small and large molecules in the pharmaceutical industry, food quality and drug screening [8-10]. The performance parameters of SPR structure include sensitivity, linearity, resolution, accuracy, reproducibility, dynamic range, the limit of detection and the limit of quantification. Advantages of surface plasmon intensification structures of SPR-based biodevices include high sensitivity, label-free, real-time, low sample consumption volume and quantitative review [10, 11].

Current researches focus on increasing the sensitivity and the stability of SPR-based biosensors to obtain more precise measurements at higher qualified and repeatable results. To meet these requirements, in the recent years, gold and silver nanoparticles (AuNP/ AgNP) and their combination have been used as the most common sensitive materials for the typical sensing layer to excite the SPR mode than the other materials with widely presented and discussed key parameters [11-14]. However, there are issues - such as the poor chemical stability, the low adsorption capacity for some molecules, the weak chemical modification ability, the broad resonance peak that reduce the accuracy and the poor biomolecular binding capacity of these sensitive layers - often limit their practical applications, specifically in terms of a device for point-of-care testing (PoCT). In recent years, SPR biosensors have very much developed and increased their sensitivity, especially in the field of PoCT, in terms of employing new detection techniques and/or using emerging materials as sensing layers such as nanoholes and quantum dots [15, 16], metallic nanoslits [17], functionalized biorecognition elements (FBRE) [18], graphene [19-22] and transition metal dichalcogenides (TMD) materials [23, 24].

Over the last two decades, graphene with 2D honeycomb structure has shown significant features in many applications from mechanical and thermal to optical and electrical. Due to its magnificent properties, graphene also has played important roles in biosensors. It can block the penetration of biomolecules; therefore, prevent the metal surfaces from the corrosion due to its dense structure. Its high surface to volume ratio promotes it to a full connection with an analyte. Graphene can bind with ligands easily and fast, and because of its high sensitivity to the carrier mobility densities, it can significantly increase the number of bindings. Also, graphene can localize SPR in Au grating resulted in sharper RI and more accurate resonance angles [19-22]. On the other hand, TMD such as molybdenum disulfide (MoS_2), with their magnificent optoelectronic features, are shown to be suitable candidates for the fabrication of the next generation of ultrasensitive biosensors. Owing relatively low cytotoxicity and genotoxicity to most of the biomolecules are also extra important key points of TMD for use in the biosensing applications. The other distinctive characteristics such as flexibility, large surface area, moderate carrier mobility, atomically thin, chemically stable and dependency of their optical and electronic properties to the number of the layers, along

with better biocompatibility and high physiological stability make them unique to improve the performance of the next generation of SPR biosensor [23-26].

The conventional structure of an SPR utilizes an active binding layer as adsorption on a planar metal, typically gold, constructed on a prism, working on the principle of optical measurement of RI changes. Despite impressive nature of gold and silver nanoparticles (AuNP and AgNP) - such as nontoxicionic, nonimmunogenic, high ratio of surface area to volume, great synthesizability, ease to functionalize and high surface chemistry - there are limitations such as interaction with some biomolecules and/or that of its capping ligands and thiol bonds in the case of functionalization. On the other hand, graphene and TMD such as MoS_2 and TaS_2 exhibit various properties - depending on their composition, crystalline structure, and the number and stacking sequence of layers – range from semiconductor to superconductor. In this paper, a stack hybrid structure consisting of different layers of MoS_2 and graphene on top of an Au layer is proposed.

Many scientific investigations, using graphene-MoS_2 hybrid structure, have been used to improve the performance of biosensors. Chowdhury et al. proposed a bilayer mirror structure consisting of graphene and MoS_2 layers, which is SPR biosensor and its performance was evaluated numerically. Based on the basic configuration, the structure with graphene and MoS_2 layers is progressively developed to improve performance. Their numerical analysis showed that by using the proposed approach, an increased sensitivity of about 4.2 times can be achieved compared to the basic Kretschmann configuration [27]. In [28], SPR biosensors based on WS_2, graphene and MoS_2 with an optimal thickness of zinc oxide, silver and $BaTiO_3$ were proposed and compared with each other. Cai et al. investigated a high-sensitivity SPR biosensor, which consists of one layer of gold, four layers of MoS_2, and single-layer grapheme [29].

This paper aims to investigate a new sensing configuration with enhanced sensitivity employing MoS_2 and graphene layers over a thin layer of gold to improve the capacity of the light absorption of the SPR biosensor and to further enhance its sensitivity. The structure is designed as an SPR biosensor at 633 nm incident light. First, the sensitivity and resonance angle of the biosensor is studied. Then, the number of layers, their thicknesses, and the order of layers are optimized for better analysis. The different structures then have been simulated in the Lumerical environment, and changes in the RI were studied and compared. The simulation is performed using a Lumerical software in the FDTD module. The FDTD method is a numerical method for solving Maxwell's equation, which is performed as a finite difference in time and space. In this analysis, two-dimensional FDTD simulation is used. The configuration of the proposed SPR biosensor is given in section 2. Results and discussion are explained in section 3. Finally, conclusions are summarized in section 4.

2. SPR BIOSENSOR STRUCTURE

Fig. 1 shows the proposed structure where different TMD and graphene layers are exploited on the Au layer, formed on a BK7 prism, and the TiO_2 layer is used as an adhesive layer between between the prism and the gold layer. Graphene has distinct electrical and optical properties. Its electronic band structure, as the main characteristic, is the factor that creates other characteristics of this material. Electrons, by moving in the honeycomb structure of graphene, lose their effective mass and become quasi-particles that obey the

Dirac equation instead of the Schrodinger equation, and this causes a different optical absorption coefficient and high electron mobility. By controlling the number of graphene layers in the biosensor structure, its performance can be optimized. A 633 nm-wavelength laser is applied to the prism where it is coupled electromagnetically with the Au layer. At convenient combinations of reflectance angle and wavelength, the appropriate layers of TMD are added to investigate a precise sensing performance in two different media: an air condition (n = 1) and when a target analyte (n = 1.02) exists. The physical properties of the different materials used for the simulation are presented in Table 1.
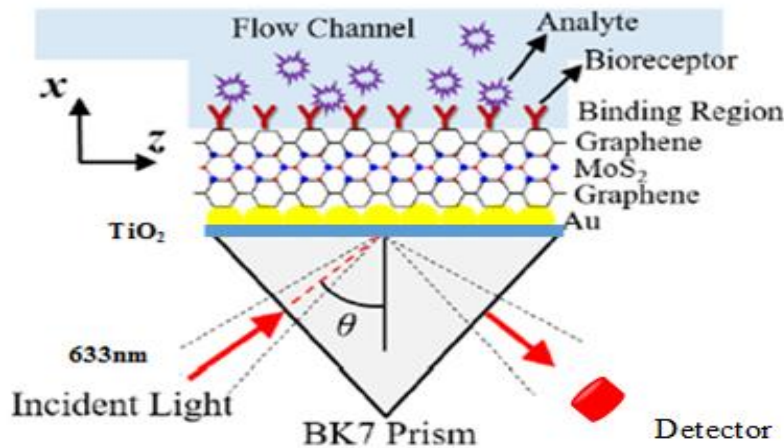

Fig. 1. Illustration of the SPR-biosensor structure, the thickness and configuration of the layers subjected to change.

Table 1. RI and thickness different layers.

Layer	Prism (BK7)	TiO$_2$	Au	MoS$_2$	Graphene
RI [30]	1.515	2.583	0.185+3.423i	5.08+1.172i	3+1.147i
Thickness	----	5 nm	10-70 nm	0.65 nm	0.34 nm

2.1. The RI of the Bioreceptor Layer

Biosensors consist of a transducer and a biosensitive part called a bioreceptor to identify biological substances. The reaction that occurs between the bioreceptor and the biological target substance causes the detection of the biological agent, and this causes the high selectivity of the biosensors. Various bioreceptors have been used in various studies, which include antibodies, enzymes, nucleic acids of DNA, RNA and aptamers, lipids, various proteins, etc [31, 32]. Bae et al. [33] used a prism made of BK7 material (n=1.5151) with the following parameters: chromium adhesive layer (5 nm), thick gold layer (43 nm), and biological receptor layer to identify Escherichia coli bacteria, as shown in Fig. 2. Imaging ellipsometry (IE) for detection of binding of Escherichia coli O157:H7 (E. coli O157:H7) to an immunosensor is reported. A protein G layer, chemically bound to a self-assembled layer of 11-mercaptoundecanoic acid (11-MUA), was adopted for immobilization of monoclonal antibody against E.coli O157:H7. The proposed SPR biosensor for the detection of Escherichia coli bacteria provides a detection range of 10^3 to 10^{7}cells/ml, as shown in the work of Bae et al., where the addition of the bioreceptor layer and the addition of 10^5 cells/ml analyte concentration increased the SPR angle in the reflection curves, this change was 1.4°.
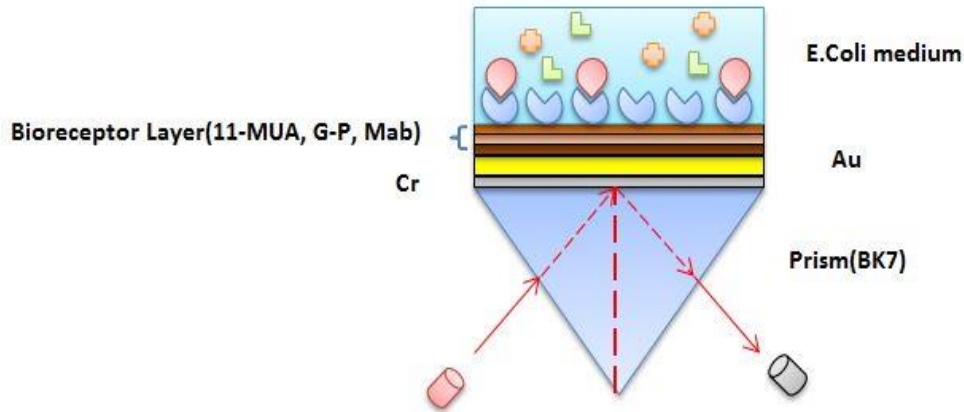
Fig. 2. Schematic of SPR biosensor.

According to the results of the work of Bae et al. [33], after the addition of biological layers, the RI of the sensing environment was changed from 1 to 1.05 with intervals of 0.005. By increasing the RI of the sensing enviroment, the angle changes according to Fig. 3. The amount of angle change is shown in Table 2. By adding 10^5 cells/ml, the RI can be estimated and as a result, its relationship with the concentration can be reached. Fig. 3 shows the reflection as a function of angle, from which the change in angle can be predicted and its linear approximation can be obtained. The SPR angle for the dry sensing environment (air) is 44°, which increases to 45.4° with an increase of 1.4°. According to Fig. 4, the linear relationship between RI and SPR angle is obtained as follows:

$$y = 66.432x - 22.42 \tag{1}$$

Based on Eq. (1), the RI of the measuring medium reaches a value of 1.02 for every 1.4° change in the SPR angle. This means that the concentration of 10^5 cells/ml of Escherichia coli will cause a change of 0.02 in the RI of the measuring medium.
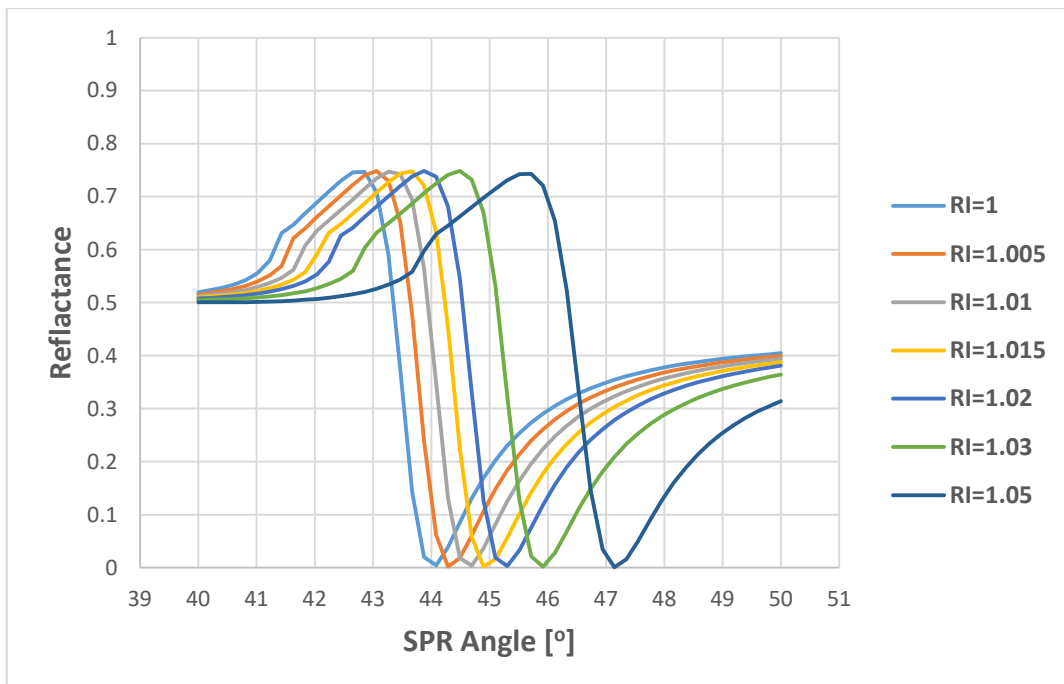

Fig. 3. Reflection as a function of SPR angle for various values of RI of the measuring medium.

Table 2. SPR angle for various values of RI of the measuring medium.

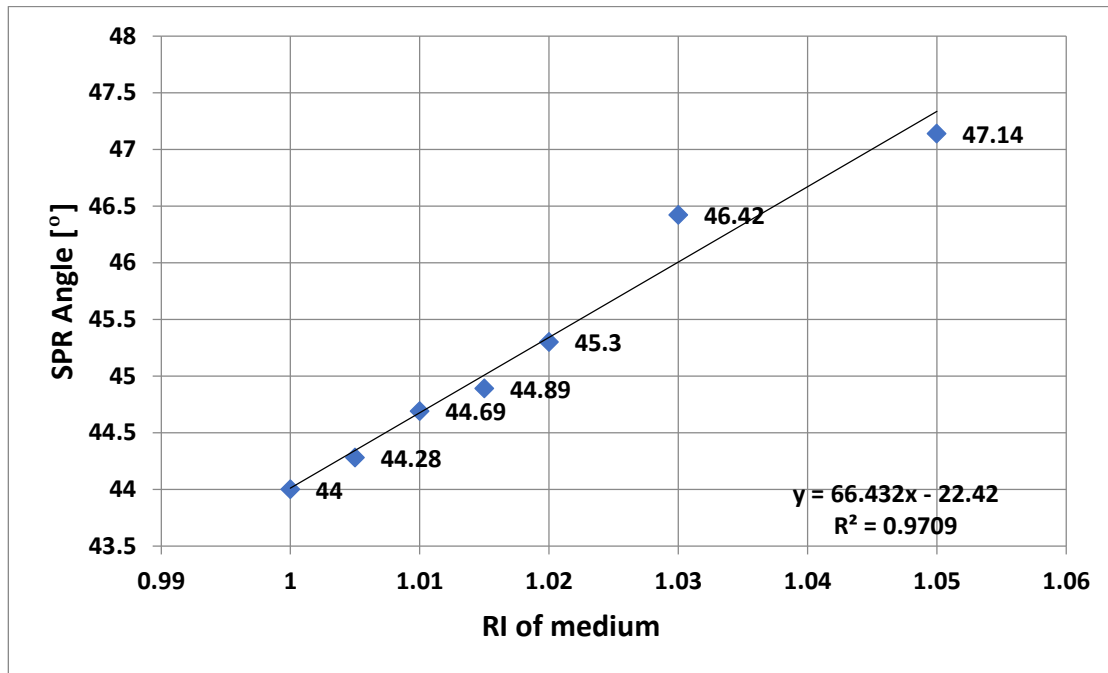| RI	1	1.005	1.01	1.015	1.02	1.03	1.05
θ_{SPR}	44	44.28	44.69	44.89	45.3	46.42	47.14

Fig. 4. SPR angle for various values of RI of the measuring medium and its linear approximation.

2.2. SPR Resonance Angle

Surface plasmon forms in the metallic-dielectric interface, known as volumetric plasmon, and propagate with the k_x wave vector in the electric metallic phase. On the other hand, the electromagnetic wave with the k wave vector descends on the surface of the prism, where k_x and k are introduced in Eqs. (2) and (3), respectively:

$$k_x = \frac{2\pi}{\lambda}\left(\frac{\varepsilon_m \varepsilon_d}{\varepsilon_m + \varepsilon_d}\right)^{1/2} \tag{2}$$

$$k = \frac{2\pi}{\lambda} n_p \sin(\theta) \tag{3}$$

where ε_m is the metal-dielectric constant, ε_d is the dielectric constant of the prism, n_p is the RI of the prism, θ is the angle of incident light descending to the prism, and λ is the wavelength of the light. If $k_x = k$, then resonance occurs and θ is defined as in Eq. (4) [34, 35]:

$$\theta = \arcsin\left[\frac{1}{n_p}\left(\left(\frac{\varepsilon_m \varepsilon_d}{\varepsilon_m + \varepsilon_d}\right)^{1/2}\right)\right] \tag{4}$$

2.3. SPR Performance Indicators

Sensitivity (S) in an SPR biosensor reflects its performance effectively,

$$S = \frac{\Delta\theta_{SPR}}{\Delta n} \tag{5}$$

where $\Delta\theta_{SPR}$ is the change in SPR angle and Δn is RI changes in the sensing medium [14].

The detection accuracy (DA) is defined as the ratio of $\Delta\theta_{SPR}$ to the full width at half maximum (FWHM) of the reflectance curve [14].

$$DA = \frac{\Delta\theta_{SPR}}{FWHM} \qquad (6)$$

The FWHM of the SPR spectra can be determined by computing the total width at half the depth of reflectance [14]. Due to the interaction between the incident light and the surface plasmon of the Au layer, at a particular angle, the incident light will minimize intensity. The aim is to find this minimum angle at given thicknesses. The lower the FWHM and the reflectance are, the more ideal and desirable the result, indicating that the surface plasmon resonance occurs more strongly. For example, Fig. 5 shows how to obtain FWHM value.
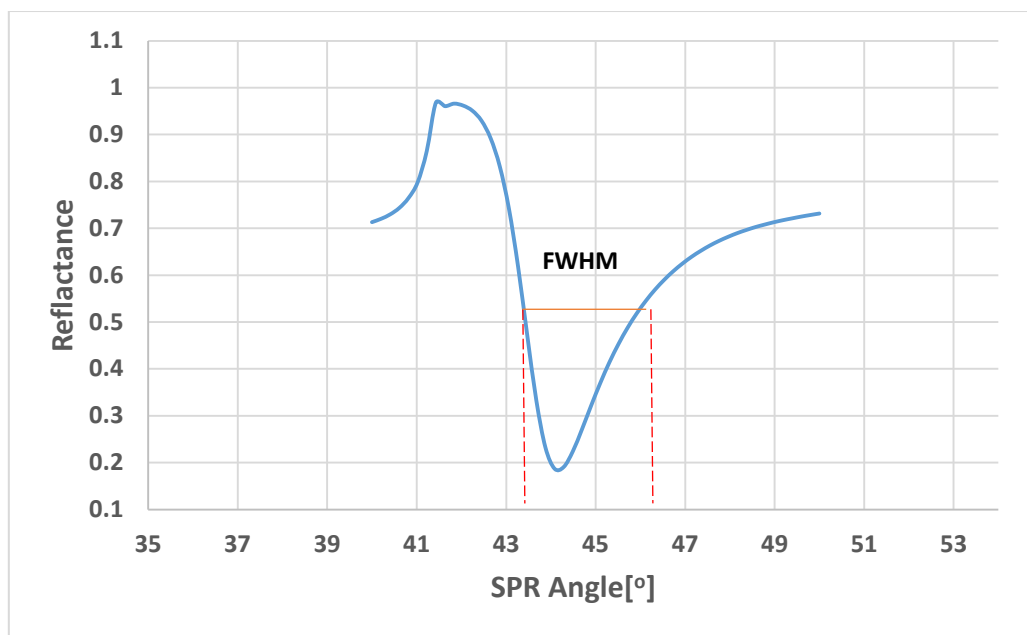

Fig. 5. FWHM of SPR curve corresponding to half from its maximum value.

Finally, the quality factor (Q) is defined as the ratio of sensitivity to the FWHM of the reflectance curve [14],

$$Q = \frac{S}{FWHM} \qquad (7)$$

3. RESULTS AND DISCUSSION

First, the effect of the single gold layer was studied by varying its thickness from 30 to 70 nm in a step of 5 nm. Fig. 6 shows the reflection responses at different thicknesses of the gold layer to 633 nm incident light.

Also, from Fig. 6, it can be realized that the optimum thickness of the Au layer is about 50~60 nm. The results of this study are presented in Table 3, in which R_{min} denotes the minimum reflectance value. It is obvious that the lowest FWHM occurs for the 60 nm Au layer and the lowest minimum reflectance value occurs for the 50 nm thick gold layer.

Because the adhesion of the Au layer to the prism is very low, we use another layer between the prism and the Au layer to increase the adhesion of the Au layer to the prism, which is a TiO_2 layer. By adding the adhesive layer (TiO2-5 nm) between the gold layer and the prism, it is observed that they reach better values.
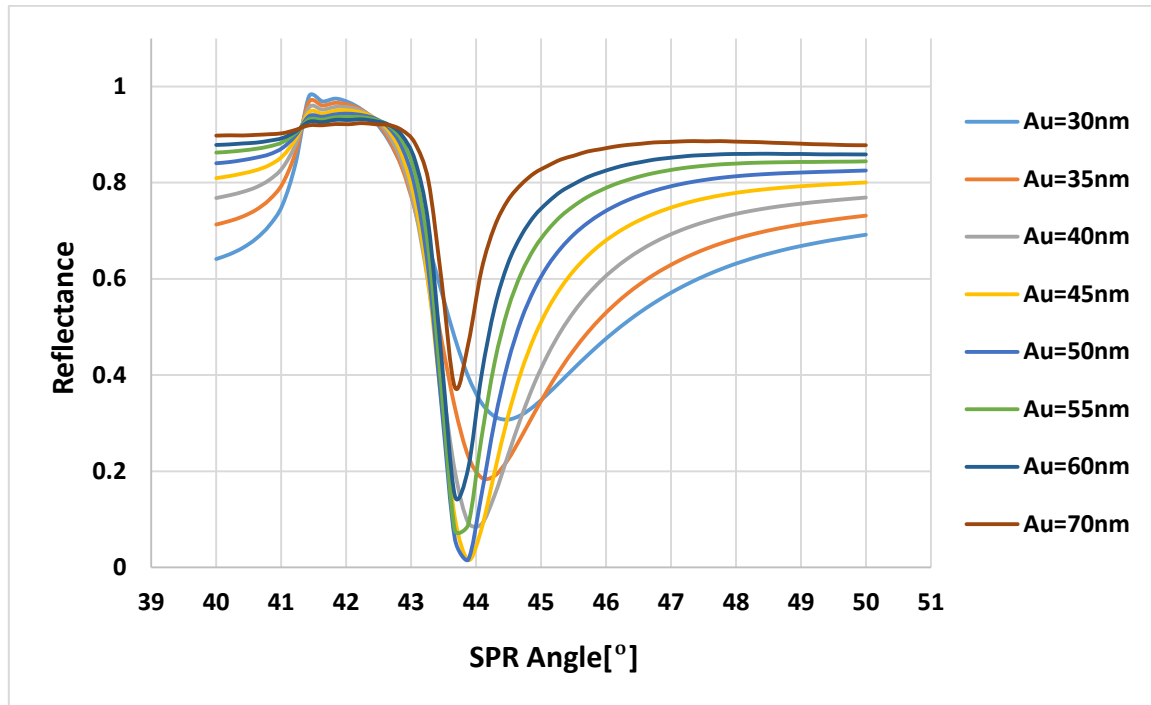

Fig. 6. Reflection curves for various values of Au layer thickness at 633 nm wavelength.

Table 3. Comparison of R_{min}, θ_{SPR} and FWHM for Au layer with various thicknesses at 633 nm wavelength.

Au thickness [nm]	R_{min}	θ_{SPR}	FWHM
30	0.30	44.48	4.81
35	0.19	44.16	3.07
40	0.09	43.99	2.14
45	0.019	43.89	1.58
50	0.016	43.87	1.28
55	0.07	43.67	1.07
60	0.15	43.67	0.66
70	0.37	43.67	0.70

We investigate the effects of the additional layers of graphene and MoS_2 on the sensitivity of the device by selecting the thickness of 50 nm for the Au layer. The configuration is first examined by adding a graphene layer above the Au layer. In order to find the optimal number of graphene layers, we add one to several layers of graphene to the previous structure and check its effect on the response of the biosensor, the results of which are shown in Fig. 7 and Table 4.
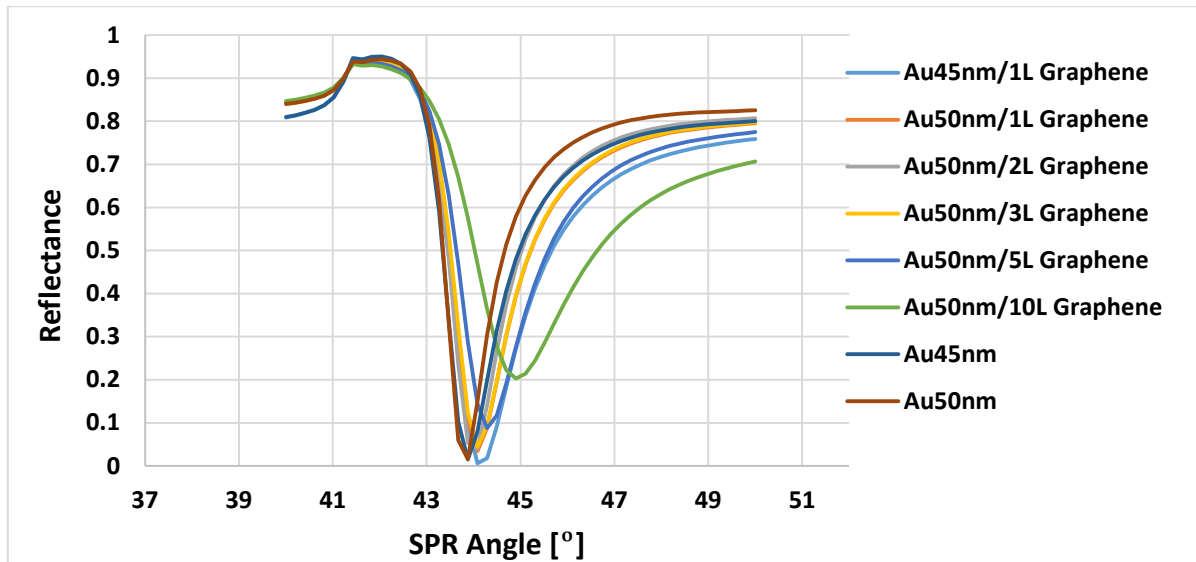
Fig. 7. Reflection curves for different thicknesses of graphene and Au at a wavelength of 633 nm.

Table 4. Comparison of R_{min}, θ_{SPR} and FWHM for the structure of BK7/Au-45,50 nm/nL Graphene and BK7/TiO2/Au-45, 50 nm/nL Graphene at a wavelength of 633 nm.

Layer	R_{min}	θ_{SPR}	FWHM
Au(45 nm)	0.019	43.89	1.58
Au(50 nm)	0.016	43.87	1.28
Au(45 nm)/1L Graphene	0.006	44.08	1.94
Au(50 nm)/1L Graphene	0.034	44.08	1.58
Au(50 nm)/2L Graphene	0.040	44.08	1.48
Au(50 nm)/3L Graphene	0.044	43.87	1.65
Au(50 nm)/5L Graphene	0.088	44.28	2.02
Au(50 nm)/10L Graphene	0.203	44.89	3.16
TiO2(5 nm)/Au(45 nm)	0.010	43.87	1.24
TiO2(5 nm)/Au(45 nm)/1L Graphene	0.008	44.08	2.14
TiO2(5 nm)/Au(45 nm)/2L Graphene	0.001	44.08	1.89
TiO2(5 nm)/Au(45 nm)/3L Graphene	0.010	44.08	2.06
TiO2(5 nm)/Au(50 nm)/1L Graphene	0.024	44.08	1.58

Also, performance parameters per 0.02 change in RI are calculated and presented in Table 5, in which Δn denotes the RI changes in the sensing medium. The results show that the sensitivity increases with the increase in the number of graphene layers.

Table 5. The effect of the number of graphene layers on the output parameters in different structures in air and bacteria environment.

Layer	Δn	$\Delta\theta_{SPR}$	FWHM	S	DA	Q
Au(50 nm)	0.02	1.232	1.28	61.6	0.78	47.65
Au(50 nm)/1L Graphene	0.02	1.22	1.58	61	0.63	38.60
Au(50 nm)/10L Graphene	0.02	1.34	3.16	67	0.31	21.20
TiO2(5 nm)/Au(50 nm)/1L Graphene	0.02	1.22	1.58	61	0.63	38.60

The results show that increasing the number of graphene layers increases the sensitivity of the biosensor. By adding ten layers of graphene, it can be seen that the sensitivity of the

biosensor increases by 9% compared to the initial state. To further increase the sensitivity and performance of the sensor, it is suggested to use other layers. Therefore, the investigation is followed up by placinga single graphene and a single MoS_2 layer and a sandwiched configuration of G/MoS$_2$/G and MoS$_2$/G/MoS$_2$ on Au layer 50 nm thickness at an air medium of n = 1. Fig. 8 depicts the corresponding spectra to the different configurations.
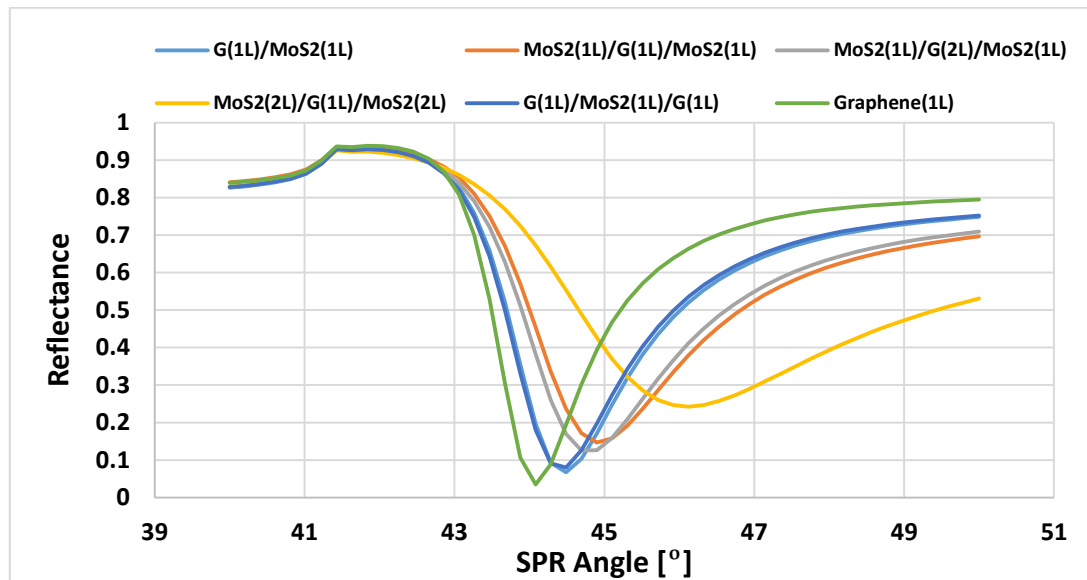

Fig. 8. Reflectance curves for graphene-MoS$_2$ hybrid configurations at 633 nm wavelength.

In the covalently bonding molybdenum (Mo) atoms between two Sulphur (S) atoms, the location of S atoms provides the metal ligand strong Au–S bonds and improves the charge transfer between S and Au. This is also true for the graphene/Au structure, that is the physisorbtion of graphene on Au, which leads to weaker bonding energies and larger equilibrium separations, the transfer of charge exists between the two. Meanwhile, the differential reflectance spectrum reveals that the presence of graphene in graphene/AuNPs significantly increases lateral scattering compared to the presence of MoS_2 in MoS$_2$/AuNPs, most likely due to much higher optical absorption coefficient of monolayer MoS_2 than the monolayer graphene, as well as the ballistic electron transportation in graphene and reduction in Fermi velocity in MoS_2 because of shifting the point in k space [36].

The reflection spectrum shown in Fig. 8 shows the minimum reflection angle as a function of the number of MoS_2 and graphene layers, which can affect the angle position, width and magnitude of the reflection. It is fully understood that the total transmittance is decreased when the number of MoS_2 flakes is increased in the structure. Although, it has already been demonstrated that an increased field-effect mobility is observed for a single layer molybdenum disulfide on graphene [37], there is no explanation yet to show the behavior of the minimum reflectance and resonance angle for the proposed sandwich configurations of the flakes in Fig. 8. One possibility is that increasing the number of molybdenum disulfide layers increases the SPR angle due to Van der Waals (vdW) interlayer coupling, which can be ascribed to Columbic interactions and potential stacking-induced changes in intralayer bonding and causes a weak electronic hybridization between the layers. Meanwhile, at a certain bonding interaction between graphene and MoS_2 flakes, a shift in

chemical potential occurs which in turns resulted in a Fermi energy pinning or linear dispersion near the gap center of MoS_2. A monolayer of MoS_2 has a thickness of around 0.65 nm, whereas graphene has a thickness of roughly 0.34 nm, without considering the impact of NPAU layer and the effect of binding of the bioreceptor layer, the effect of thickness of a monolayer MoS_2 on a monolayer of graphene could be speculated at 1:2 in the structure. Increasing the number of MoS_2 flakes above two causes a dramatic degradation in the minimum reflectance. As previously demonstrated in Table 1, the alteration may be interpreted as a large real value and a small imaginary part of MoS_2's dielectric constant, which is ascribed to the low electron energy loss.

Performance parameters per 0.02 change in RI for presenting about 10^5 cells/mL E.Coli, are calculated and presented in Table 6. The results show that adding the MoS_2 layer increases the sensitivity in the biosensor, which is the highest value for the MoS_2-1L/Graphene-2L/MoS_2-1L configuration and is equal to 71.5 °/RIU. This increase in sensitivity compared to the initial state is 17.5%, but at the same time, the detection accuracy is reduced. The results of other researches on sensors designed based on graphene are also presented in Table 7 for further comparison.

Table 6. Effect of the hybrid structure of graphene andMoS_2on on the output parameters in different structures in air and bacteria environment.

Layer	Δn	$\Delta\theta_{SPR}$	FWHM	S	DA	Q
TiO_2/Au/1L Graphene	0.02	1.22	1.58	61	0.63	38.60
TiO_2/Au/1L G/1L MoS_2	0.02	1.23	2.27	61.5	0.44	27.09
TiO_2/ Au/1L MoS_2/1L G/1L MoS_2	0.02	1.31	3.28	65.5	0.30	19.96
TiO_2/ Au/1L MoS_2/2L G/1L MoS_2	0.02	1.43	2.99	71.5	0.33	23.91
TiO_2/ Au/2L MoS_2/1L G/2L MoS_2	0.02	1.32	6.77	66	0.14	9.74
TiO_2/ Au/1L G / 1L MoS_2/1L G	0.02	1.23	2.06	61.5	0.48	29.85

Table 7. Performance paprameters for graphene-based SPR sensors.

Configuration	Wavelength [nm]	S [°RIU^{-1}]	DA	Q [RIU^{-1}]	References
Prism/TiO_2/Au/MoS_2-1L/Graphene-2L/MoS_2-1L	633	71.5	0.33	23.91	This work
Prism/Au/Si/Graphene	632	53.75	0.05	---	[38]
Prism/Au /MoS_2/Graphene/BRE	632.8	45.97	0.30	2.52	[39]
Prism/Au/Graphene/Anity Layer	633	33.98	0.29	2.78	[40]

4. CONCLUSIONS

In this work, the effect of different MoS_2/graphene/Au combination and the numbers of their flakes on the spectral response of an SPR-biosensor was numerically studied and presented. Furthermore, a comparison on the orders and thicknesses of the MoS_2/graphene heterostructure to the medium was performed. We also analyzed the sensitivity and other parameters of the sensor to obtain the best configuration feature. The results showed that the 1L_MoS_2(0.65 nm)/2L_G(0.68 nm)/1L_MoS_2 (0.65 nm) on 50 nm Au/5 nm TiO_2/Prism possesses the highest sensitivity of 71.5 °/RIUper 10^5 cells/ml of Escherichia coli bacteria. The results also indicated that increasing the number of layers in the heterostructure in the output has a direct effect on the sensor performance. On the basis of the results from the

improved configuration of the proposed model, it is anticipated that a new potential for an SPR biosensor with very high performance for the detection of the bacteria may exist.

REFERENCES

[1]   W. Murray, W. Barnes, "Plasmonic materials," *Advanced Materials*, vol. 19, no. 22, pp. 3771-3782, 2007.

[2]   S. Kawata, M. Ozaki, "Surface-plasmon holography," *IScience*, vol. 23, no. 12, pp. 101879, 2020.

[3]   J. Homola, I. Koudela, S. Yee, "Surface plasmon resonance sensors based on diffraction gratings and prism couplers: sensitivity comparison," *Sensors and Actuators B: Chemical*, vol. 54, no. 1-2, pp. 16-24, 1999.

[4]   L. Wu, H. Chu, W. Koh, E. Li, "Highly sensitive graphene biosensors based on surface plasmon resonance," *Optics Express*, vol. 18, no. 14, pp. 14395-14400, 2010.

[5]   P. Maharana, R. Jha, "Chalcogenide prism and graphene multilayer based surface plasmon resonance affinity biosensor for high performance," *Sensors and Actuators B: Chemical*, vol. 169, pp. 161-166, 2012.

[6]   A. Komlev, R. Dyukin, E. Shutova, "The method of controlling the thickness of the deposited film on the basis of the surface plasmon resonance effect," *Journal of Physics: Conference Series*, vol. 872, no. 1, pp. 012042, 2017.

[7]   R. Verma, B. Gupta, R. Jha, "Sensitivity enhancement of a surface plasmon resonance based biomolecules sensor using graphene and silicon layers," *Sensors and Actuators B: Chemical*, vol. 160, no. 1, pp. 623-631, 2011.

[8]   H. Gwon, S. Lee, "Spectral and angular responses of surface plasmon resonance based on the Kretschmann prism configuration," *Materials Transactions*, vol. 51, no. 6, pp. 1150-1155, 2010.

[9]   J. Homola, "Surface plasmon resonance sensors for detection of chemical and biological species," *Chemical Reviews*, vol. 108, no. 2, pp. 462-493, 2008.

[10] N. Cennamo, F. Chiavaioli, C. Trono, S. Tombelli, A. Giannetti, F. Baldini, L. Zeni, "A complete optical sensor system based on a POF-SPR platform and a thermo-stabilized flow cell for biochemical applications," *Sensors*, vol. 16, no. 2, pp. 196, 2016.

[11] X. Zhao, T. Huang, P. Ping, X. Wu, P. Huang, J. Pan, Y. Wu, Z. Cheng, "Sensitivity enhancement in surface plasmon resonance biochemical sensor based on transition metal dichalcogenides/graphene heterostructure," *Sensors*, vol. 18, no. 7, pp. 2056, 2018.

[12] C. Rizal, V. Belotelov, "Sensitivity comparison of surface plasmon resonance (SPR) and magneto-optic SPR biosensors," *The European Physical Journal Plus*, vol. 134, no. 9, pp. 435, 2019.

[13] X. Dai, Y. Liang, Y. Zhao, S. Gan, Y. Jia, Y. Xiang, "Sensitivity enhancement of a surface plasmon resonance with Tin Selenide (SnSe) allotropes," *Sensors*, vol. 19, no. 1, pp. 173, 2019.

[14] L. Wu, Y. Jia, L. Jiang, J. Guo, X. Dai, Y. Xiang, D. Fan, "Sensitivity improved SPR biosensor based on the MoS2/graphene–aluminum hybrid structure," *Journal of Lightwave Technology*, vol. 35,   no. 1, pp. 82-87, 2016.

[15] A. Prasad, J. Choi, Z. Jia, S. Park, M. Gartia, "Nanohole array plasmonic biosensors: emerging point-of-care applications," *Biosensors and Bioelectronics*, vol. 130, pp. 185-203, 2019.

[16] L. Niu, K. Cheng, Y. Wu, T. Wang, Q. Shi, D. Liu, Z. Du, "Sensitivity improved plasmonic gold nanoholes array biosensor by coupling quantum-dots for the detection of specific biomolecular interactions," *Biosensors and Bioelectronics*, vol. 50, pp. 137-142, 2013.

[17] C. Ge, Z. Guo, Y. Sun, F. Shen, Y. Tao, J. Zhang, R. Li, L. Luo, "Spatial and spectral selective characteristics of the plasmonic sensing using metallic nanoslit arrays," *Optics Communications*, vol. 359, pp. 393-398, 2016.

[18] J. Qu, A. Dillen, W. Saeys, J. Lammertyn, D. Spasic, "Advancements in SPR biosensing technology: an overview of recent trends in smart layers design, multiplexing concepts, continuous monitoring and in vivo sensing," *Analytica Chimica Acta*, vol. 1104, pp. 10-27, 2020.

[19] C. Zhang, Z. Li, S. Jiang, C. Li, S. Xu, J. Yu, Z. Li, M. Wang, A. Liu, B. Man, "U-bent fiber optic SPR sensor based on graphene/AgNPs," *Sensors and Actuators B: Chemical*, vol. 251, pp. 127-133, 2017.

[20] Z. Sadeghi, H. Shirkani, "Highly sensitive mid-infrared SPR biosensor for a wide range of biomolecules and biological cells based on graphene-gold grating," *Physica E: Low-Dimensional Systems and Nanostructures*, vol. 119, pp. 114005, 2020.

[21] M. Hossain, I. Mehedi, M. Moznuzzaman, L. Abdulrazak, M. Hossain, "High performance refractive index SPR sensor modeling employing graphene tri sheets," *Results in Physics*, vol. 15, pp. 102719, 2019.

[22] X. Sheng, J. Liu, H. Yang, L. Chen, J. Li, H. Liu, "Optimization of tunable symmetric SPR sensor based on Ag-graphene," *Optik*, vol. 184, pp. 339-347, 2019.

[23] H. Hu, A. Zavabeti, H. Quan, W. Zhu, H. Wei, D. Chen, J. Ou, "Recent advances in two-dimensional transition metal dichalcogenides for biological sensing," *Biosensors and Bioelectronics*, vol. 142, pp. 111573, 2019.

[24] G. Vibisha, J. Nayak, P. Maheswari, N. Priyadharsini, A. Nisha, Z. Jaroszewicz, K. Rajesh, R. Jha, "Sensitivity enhancement of surface plasmon resonance sensor using hybrid configuration of 2D materials over bimetallic layer of Cu–Ni," *Optics Communications*, vol. 463, pp. 125337, 2020.

[25] M. Rahman, M. Anower, M. Hasan, M. Hossain, M. Haque, "Design and numerical analysis of highly sensitive Au-MoS$_2$-graphene based hybrid surface plasmon resonance biosensor," *Optics Communications*, vol. 396, pp. 36-43, 2017.

[26] K. Sreekanth, S. Zeng, K. Yong, T. Yu, "Sensitivity enhanced biosensor using graphene-based one-dimensional photonic crystal," *Sensors and Actuators B: Chemical*, vol. 182, pp. 424-428, 2013.

[27] S. Chowdhury, S. Uddin, E. Kabir, "Numerical analysis of sensitivity enhancement of surface plasmon resonance biosensors using a mirrored bilayer structure," *Photonics and Nanostructures - Fundamentals and Applications*, vol. 41, pp. 100815, 2020.

[28] A. Kumar, A. Yadav, A. Kushwaha, S. Srivastava, "A comparative study among WS2, MoS$_2$ and Graphene based surface plasmon resonance (SPR) sensor," *Sensors and Actuators Reports*, vol. 2, no. 1, pp. 100015, 2020.

[29] H. Cai, M. Wang, Z. Wu, J. Liu, X. Wang, "Performance enhancement of SPR biosensor using Graphene-MoS$_2$ hybrid structure," *Nanomaterials*, vol. 12, no. 13, pp. 2219, 2022.

[30] P. Johnson, R. Christy, "Optical constants of the noble metals," *Physical Review B*, vol. 6, no. 12, pp. 4370, 1972. <https://refractiveindex.info>

[31] S. Lim, M. Ahmed, *Chapter 1: Introduction to Food Biosensors*, Royal Society of Chemistry, 2017.

[32] A. Krissanaprasit, C. Key, S. Pontula, T. Labean, "Self-assembling nucleic acid nanostructures functionalized with aptamers," *Chemical Reviews*, vol. 121, no. 22, pp.13797-13868, 2021.

[33] Y. Bae, K. Park, B. Oh, J. Choi, "Immunosensor for detection of Escherichia coli O157: H7 using imaging ellipsometry," *Journal of microbiology and biotechnology*, vol. 16, no. 8, pp. 1169-1173, 2006.

[34] H. Raether, "Surface plasmons on smooth surfaces, in Surface plasmons on smooth and rough surfaces and on gratings," *Springer*, pp. 4-39, 1988.

[35] K. Choi, H. Kim, Y. Lim, S. Kim, B. Lee, "Analytic design and visualization of multiple surface plasmon resonance excitation using angular spectrum decomposition for a Gaussian input beam," *Optics Express*, vol. 13, no. 22, pp. 8866-8874, 2005.

[36] C. Backes, A. Abdelkader, C. Alonso, A. Andrieux-Ledier, R. Arenal, J. Azpeitia, N. Balakrishnan, L. Banszerus, J. Barjon, R. Bartali, S. Bellani, "Production and processing of graphene and related materials," *2D Materials*, vol. 7, no. 2, pp. 022001, 2020.

[37] G. Lee, Y. Yu, X. Cui, N. Petrone, C. Lee, M. Choi, D. Lee, C. Lee, W. Yoo, K. Watanabe, T. Taniguchi, "Flexible and transparent MoS_2 field-effect transistors on hexagonal boron nitride-graphene heterostructures," *ACS Nano*, vol. 7, no. 9, pp. 7931–7936, 2013.

[38] N. Zhang, G. Humbert, T. Gong, P. Shum, K. Li, J. Auguste, Z. Wu, D. Hu, F. Luan, Q. Dinh, M. Olivo, "Side-channel photonic crystal fiber for surface enhanced Raman scattering sensing," *Sensors and Actuators B: Chemical*, vol. 223, pp. 195-201, 2016.

[39] J. Maurya, Y. Prajapati, V. Singh, "Performance of graphene–MoS 2 based surface plasmon resonance sensor using Silicon layer," *Optical and Quantum Electronics*, vol. 47, no. 11, pp. 3599-3611, 2015.

[40] A. Verma, A. Prakash, R. Tripathi, "Performance analysis of graphene based surface plasmon resonance biosensors for detection of pseudomonas-like bacteria," *Optical and Quantum Electronics*, vol. 47, no. 5, pp. 1197-1205, 2015.